JOURNAL OF MATERIALS SCIENCE 13 (1978) 1740–1748

High temperature creep behaviour of nearly stoichiometric alumina spinel

R. DUCLOS*, N. DOUKHAN, B. ESCAIG
Laboratoire de Structure et Propriétés de l'Etat Solide†, Université des Sciences et Techniques de Lille, B.P. 36, 59650 Villeneuve d'Ascq, France

Creep behaviour of nearly stoichiometric spinel, $(Al_2O_3)_n$ MgO, $n = 1.1$, is investigated for compression axis [0 0 1], at temperatures 0.77 to 0.83 T_m and constant loads 88.2 to 117.6 MPa. Experimental observations, including the mechanical creep law and the dislocation substructures as imaged by TEM and Berg-Barrett X-ray topography support the following picture: {1 0 0}⟨1 1 0⟩ slip is activated in the very early creep stage, while no evidence for {1 1 1} is found; on the other hand {1 1 1} slip planes are observed for stress orientation [1 1 0], in agreement with Schmid's law. (ii) When in edge orientation slip dislocations become sessile by pure climb splitting. Their dissociation plane has been determinated unambiguously and observed to be perpendicular to their Burgers vector. As a result, it is suggested that slip should be inhibited and further creep should occur by pure climb strain only. This expected "climb–creep" accounts for experimental rates and, tentatively, for their dependence on stoichiometry n since the latter is observed to change only pre-exponential terms, the creep energies being much the same whatever the value of n.

1. Introduction

The plasticity of alumina spinel solid solutions, $(Al_2O_3)_n$ MgO, raises the basic problem of {1 1 1}⟨1 1 0⟩ "metallic" slip versus {1 1 0}⟨1 1 0⟩ "ionic" slip in oxide crystals, since it has been claimed [1–4] that both could be produced in this system, depending on the stoichiometry or molar ratio, n. While crystals with $n \simeq 2$ are relatively easy to deform [2, 3, 5], and show clearly a {1 1 0}⟨1 1 0⟩ slip, the deformation behaviour of stoichiometric crystals ($n = 1$) is much less documented owing to their difficult growth and the quite strong resistance they oppose to plastic shear, being brittle up to at least $0.75\,T_m$ ($T_m = 2408$ K). Single crystal data have been limited, for $n = 1$, to constant strain rate compression tests, performed at $T \geqslant 0.8\,T_m$ in two orientations only, both favouring a {1 1 1}⟨1 1 0⟩ slip. This slip has thus been shown at low strains (smaller than a few per cent) by Radford *et al.* [2] by etch-pitting, for a Schmid factor ratio (SFR) on (1 1 1) versus (1 1 0) of 0.41/0.25 = 1.64, and by Mitchell *et al.* [4] by slip line and electron microscopy observations, for a SFR of 0.5/0.35 = 1.43 in the range 0.86 to $0.90\,T_m$. From these data, it is stated that {1 1 1} slip would characterize the stoichiometry $n = 1$. The latter authors attribute the high strength of $n = 1$ crystals to a large Peierls force on {1 1 1} planes, assuming a still higher one to exist on {1 1 0} planes; the transition to {1 1 0} slip as n increases from 1 to 2 would then follow from a steeper hypothetic lowering of Peierls barriers on {1 1 0} than on {1 1 1} planes, owing to the diffusion of the excess cation vacancies.

We present here a somewhat different picture based on the creep behaviour of nearly stoichiometric crystals, $n \simeq 1.1$, stressed along [0 0 1] which favours {1 1 0}⟨1 $\bar{1}$ 0⟩ slip (SFR, on {1 1 1} versus {1 $\bar{1}$ 0}, is 0.41/0.5 = 0.82), at temperatures between 0.77 and $0.83\,T_m$. The mechanical creep

*This paper is part of the work done by RD for a Thèse d'Etat dissertation.

†Associated with CNRS.

law, and the dislocation substructures have been investigated by transmission electron microscopy (TEM) and Berg-Barrett X-ray topography (BBT). In the course of this investigation, it has been made possible to determine for the first time unambiguously the dissociation plane of slip dislocations, and to show that they dissociate in a sessile way, normally to their Burgers vector, in the early stage of creep. Consequently, the actual dissociation width has been obtained. Other information on active slip planes, which are found to be $\{1\,1\,0\}$ and not $\{1\,1\,1\}$, and on the relations between stoichiometry and plastic behaviour, can be deduced which do not support all the preceding views.

2. Experimental procedures

Compression specimens 2.5 mm × 2.5 mm × 6 mm were cut with a diamond saw from a Verneuil grown single crystal of stoichiometry $n \simeq 1.1$ purchased from Cristal-Tec/LETI (Grenoble). They contained only a few p.p.m. of impurities, principally Ca^{2+} and Fe^{3+}.

Specimens were then mechanically polished, and crept along the compression axis [0 0 1] at temperatures 1848 to 2003 K, in air inside a graphite furnace. A constant load, 88.2 to 117.6 MPa, was applied on a dead weight creep machine, of the type described in [5].

After creep tests, creep substructures were observed by BBT or TEM. All Berg-Barrett topographs were taken after polishing off the sample surfaces at about a 100 μm depth, or after sawing inside the sample itself, to be representative of the bulk (for more details and the understanding of topograph contrast, see [5]). Thin foils for TEM were prepared by ionic bombardment and examined at 100 kV.

3. Experimental results

3.1. Mechanical creep law

Some creep curves are given in Fig. 1. Only nominal stress is kept constant during tests, because of the low strain values, and the unusual shape of crept specimens (inverted barrel). Some observation on $\epsilon(t)$ curves deserve attention:

(i) they do not show any transient creep, which would correspond to an initial decrease of strain rate.

(ii) since the strain obtained under constant load is linear in time, under a constant true stress it would be slightly accelerated. What we observe in Fig. 1 is therefore only quasi steady state creep.

(iii) the reproducibility of tests is poor, the strain rate being reproduced only within a factor two.

These features are easier to understand as a pure climb strain, possibly nucleation-controlled, than as the usual glide strain process, controlled by propagation through obstacles.

The observed creep rate is very low, smaller by a factor about 50 than creep under comparable conditions of samples with a different stoichiometry, e.g. $n = 1.8$, as measured in [5] and [6]. However the Arrhenius plot in Fig. 2 shows this factor comes in pre-exponential terms only, and not in activation energies, the slopes being much the same. Thus, the creep law is found to be:

$$\dot{\epsilon} = \dot{\epsilon}_0 \, (\sigma/\mu)^m \exp(-U/kT) \qquad (1)$$

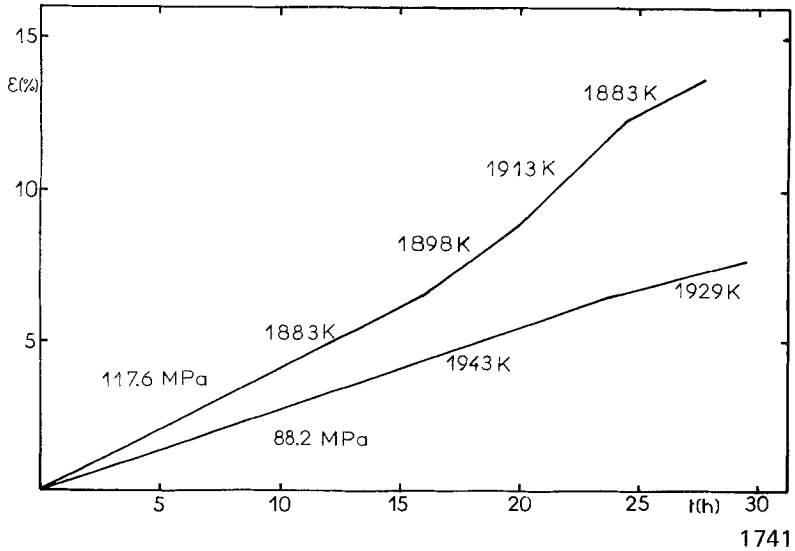

Figure 1 Creep curves for the [0 0 1] orientation at 117.6 and 88.2 MPa for temperature change experiments.

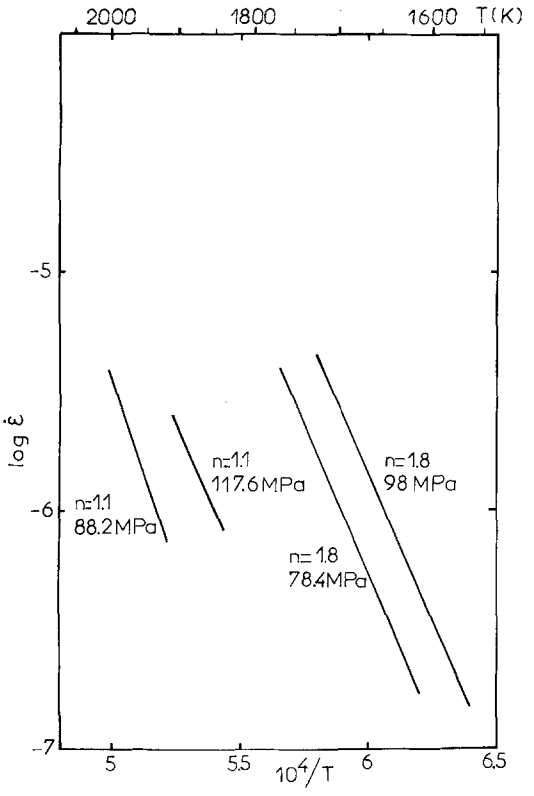

Figure 2 Arrhenius plot of creep rate versus T for stoichiometries $n = 1.1$ (this work) and $n = 1.8$ (from [5]).

with $m \simeq 4 \pm 0.5$ and $U = 5.7 \pm 0.7$ eV, as determined by stress or temperature jumps ($\Delta\sigma = \pm 10$ MPa, $\Delta T = \pm 15$ K). These values are quite similar to corresponding figures found in [5] for the stoichiometry $n = 1.8$: $U = 5.3 \pm 0.5$ eV and $m = 3.9 \pm 0.3$ (or also in [6] at higher temperatures). In the same trend, recent measurements by Ando and Oishi [8] of self-diffusion coefficients for oxygen ions (shown to be the slowest moving species in spinels) show no influence of stoichiometry on diffusion parameters for $n = 1$ and $n = 2.2$. Therefore, it is clearly established that the large differences in creep strength are not related to hypothetical differences in self-diffusion processes. The same probably holds true also for any kind of high temperature mechanical strength, e.g. yield stress contrary to a number of previous suggestions [2, 4].

A last observation is of interest, in connection with a possible climb strain process. While barrel-shaped samples are always obtained after compression in the case $n = 1.8$, with one of the transverse dimension kept unchanged (i.e. plane strain conditions), an unusual concave shape (inverted barrel) is always obtained in the case $n = 1.1$. Moreover, specimen sections are clearly widened in both of the transverse directions. Microprobe stoichiometry analysis gives nearly no variation of n across the sample ($n = 1.1 \pm 0.1$), ruling out any possible diffusion of alumina from the alumina buttons used to prevent indentations. This shape change can only be produced either by a rather difficult to accept multiple glide process, involving at least four intersecting active glide systems, or more plausibly by a diffusion climb process. At corners in particular, there may be vacancy concentration gradients stronger than elsewhere because of stress concentrations and/or the proximity of available surface diffusion sinks and sources; such gradients are expected to produce the kind of inverted barrel shape which is observed.

3.2. Creep substructures

Quite generally, slip substructures are difficult to observe after high temperature creep. In our case, strain rates are in the range 10^{-6} sec^{-1} so that it takes about 30 h at $0.8\,T_m$ to reach a 10% strain. It is clear that only recovery substructures, e.g. climb polygonization, can survive to such a long run [18].

Whatever the creep mechanism, possible slip features can only be expected after a short creep time, i.e. a low creep strain. Therefore we present below two types of results: firstly, substructures left after less than an hour creep, corresponding to a 0.2 or 0.3% strain, and substructures left after a ten hour creep (or more), corresponding to a 5 to 13% strain.

3.2.1. Short time substructures

After a 0.3% creep strain, Berg-Barrett topographs of the two side faces of the sample are quite similar. One of them is shown in Fig. 3a, where extinction contrast (locally, some displacement contrast too) features [1 0 0] lines (and [0 1 0] on the (1 0 0) face). TEM helps in interpretation of these lines (see below), but it is already clear that they cannot be compatible with any {1 1 1} slip. Of course, it could be argued that no slip at all exists in our creep conditions. Nevertheless, we have observed such a {1 1 1} slip on topographs taken on similar samples, after similar creep strain and similar creep conditions but with a [1 1 0] compression axis which favours this slip over the {1 1 0} one (SFR = 1.64). This is shown in Figs. 3b

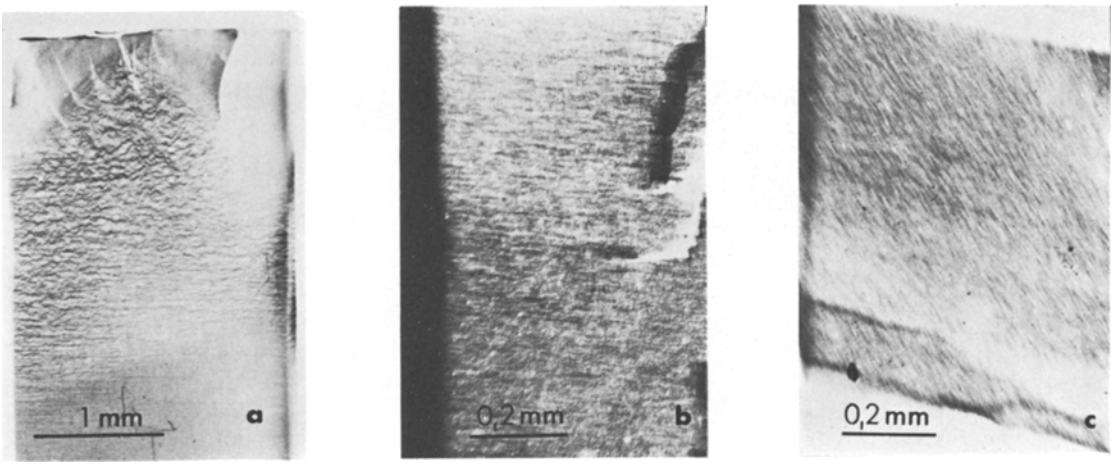

Figure 3 (a) BBT of the (0 1 0) face of a [0 0 1] compression specimen with $n = 1.1$., after 0.3% creep strain at 107.8 MPa and 1853 K. $\mathbf{g} = [6\,6\,0]$. (b) BBT of the (0 0 1) face of a [1 1 0] compression specimen with $n = 1.1$. after 0.3% creep strain at 117.6 MPa and 1903 K. $\mathbf{g} = (\bar{4}\,0\,4)$. (c) Same sample as (b). $(1\,\bar{1}\,0)$ face. $\mathbf{g} = (4\,0\,4)$. Owing to the distortion the angle between the [1 1 2] direction and the [1 1 0] compression axis is 40°.

and c for comparison. Therefore we think that slip does exist in the early stage of creep we observe, and this slip cannot be of the type {1 1 1}. On the other hand, slip is specific to the very early stage and should not develop much further than a few 10^{-3} strain (say, in the first creep hour) to account for the mechanical behaviour described in Section 3.1, and for observations of the long time substructures.

Samples deformed 0.2% under 117.6 MPa at 1848 K have been observed by TEM. Dislocation density is low, of the order 10^{11} m^{-2}, but it consists of a number of long straight edge dislocations lying along [0 1 0] and [1 0 0], quite frequently observed and homogeneously distributed throughout the foil (at this very small scale), as is shown typically in Fig. 4a. Their slip plane is observed to belong to the four most stressed {1 1 0} planes, giving thus strong support to a {1 1 0} slip. No evidence for {1 1 1} slip is found either. This suggests that the above topograph (Fig. 3a) could represent the [1 0 0] dislocation family, distributed as a series of rough sheets at the sample scale (which is the BBT scale). Of course the other family, along [0 1 0], is also present and should be in contrast for the topograph diffraction vector $\mathbf{g} = [6\,6\,0]$. Beneath the (0 1 0) face, and within the near surface region, say a few μm thick, which is effectively diffracting, the short bits of [0 1 0] (1 0 1) sheets are viewed edge-on and are not distinguishable from the [1 0 0] (0 1 1) sheets which lie in contrary to their full length along it. The only effect seen is the cusps (displacement contrasts) visible on [1 0 0] contrast lines. Only one family is clearly visible on each face: [1 0 0] on the (0 1 0), [0 1 0] on the (1 0 0) face.

The presence of these straight dislocations, relatively widely spaced, has made it possible to determine unambiguously their dissociation plane by standard stereographic methods. Using weak beam images, it has been found they are dissociated into two collinear partials, of Burgers vector 1/4 [1 0 1], in plane (1 0 1), i.e. normal to their slip plane.

Let δ be the apparent partial separation, as measured on the micrograph plane P, d the true dissociation width, d_p the projection of d onto P, and l_p the unit line vector along the projected partials onto P. Let the angles ϕ and χ be defined as: $\phi = (d_p, l_p)$, $\chi = (d, d_p)$. Simple geometry gives the relation:

$$d = \delta (\sin \phi \cos \chi)^{-1}$$

Apparent separations δ are then carefully measured (using a microdensitometer) for a series of weak beam images taken for various tilt angles (ranging between $+47°$ and $-41°$). An example is given in Fig. 4b, where the partial separation δ is about 8 nm. Special care is taken in keeping rigorously the same weak beam diffraction conditions and the same calibrated magnification on the microscope (M 19 on Philips E.M. 300) while tilting is performed. Weak beam geometry corresponds to that defined by Cockayne [9], i.e. $s_g \geqslant 0.2\,\text{nm}^{-1}$

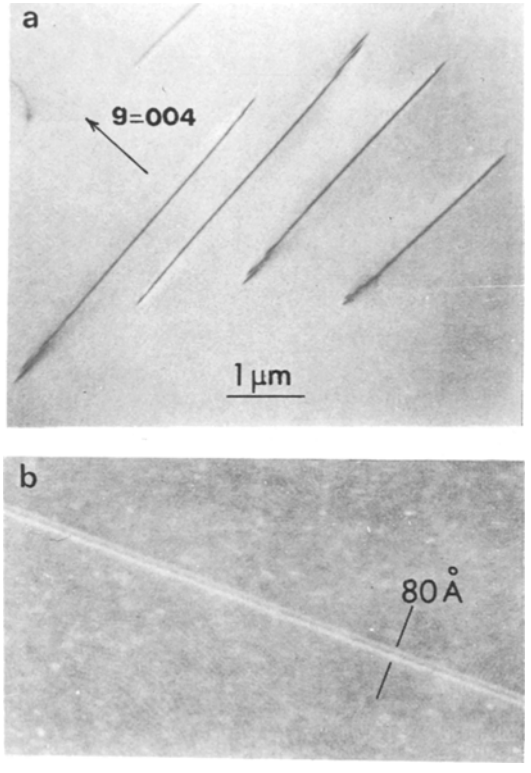

Figure 4 (a) (1 0 0) section. Straight edge dislocations along [0 1 0] are characteristic of the creep substructure at 0.2% strain. Sample deformed at 1848 K and 117.6 MPa, with a [0 0 1] compression axis. (b) Partial separation of an edge dislocation as in (a).

and $|s_g \xi_g| \geqslant 5$; we use $\mathbf{g} = [0\,4\,4]$, with the bright Kikuchi line on [0 8 8], that is: $s_g \simeq 0.2\,\mathrm{nm}^{-1}$ and $|s_g \xi_g| = 17$ ($\xi_g = 85$ nm for [0 4 4]).

The experimental plot of δ versus the tilt angle θ is then compared to variations $\delta(\theta)$ computed for various plausible dissociation planes, in zone with the line vector [0 1 0]. Fig. 5 shows that only the (1 0 1) plane fits the experimental data. This means that edge dislocations are dissociated not in their glide plane (which is (1 0 $\bar{1}$)) but in the plane perpendicular to their Burgers vector. This kind of splitting involves pure climb. At creep temperatures, it is obvious that a true equilibrium width can be reached. This one is found to be $d \simeq 10 \pm 1$ nm.

The corresponding stacking fault, (1 0 1) 1/4 [1 0 1], is obviously one of the less energetic faults since not only it does not perturb the oxygen anion sublattice but it changes only one ionic plane (parallel to the fault) every two planes; moreover the two half crystals from each side of the fault plane are in a twin configuration. It has been predicted as the lowest energy fault by Van der Biest *et al.*, and observed by them in lithium ferrite spinel [10], and by Veyssiere *et al.* [11] who showed it should be particularly stabilized in inverse or cation disordered spinels, as can be expected to occur in our high temperature case. Taking as the smallest lattice repeat period $b \simeq 0.58$ nm, the shear modulus $\mu \simeq 1.18 \times 10^5$ MPa, and the Poisson ratio $\nu \simeq 0.25$, the measured width d corresponds to a stacking fault energy:

$$\gamma = \mu b/325 = 215\,\mathrm{mJ\,m^{-2}}$$

Predictions by Veyssiere *et al.* [11] would give in our case $\gamma = 1329\,\mathrm{mJ\,m^{-2}}$, a number about 6 times larger than the experimental value.

To conclude this section, experimental evidence supports the following picture: in the very early stage of creep, dislocations start bowing out under the applied stress and slip on the most stressed plane, (1 0 1) in our case, until they take on an edge character. Once edge, they become sessile by climb dissociation into two collinear partials so that they

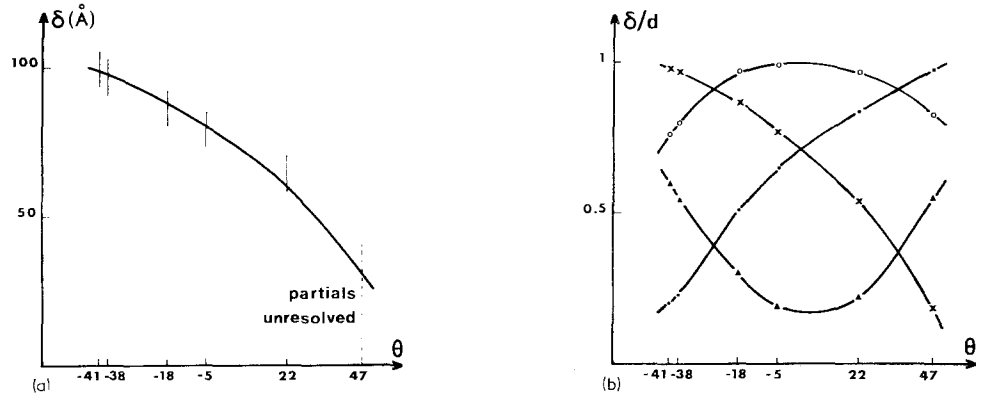

Figure 5 (a) Experimental variation $\delta(\theta)$ of partial separation δ versus tilt angle (θ). (b) Computed variations $\delta(\theta)$ for various plausible dissociation planes: × (1 0 1); • (1 0 $\bar{1}$); ○ (1 0 0); ▲ (0 0 1). Only the (1 0 1) plane fits the data.

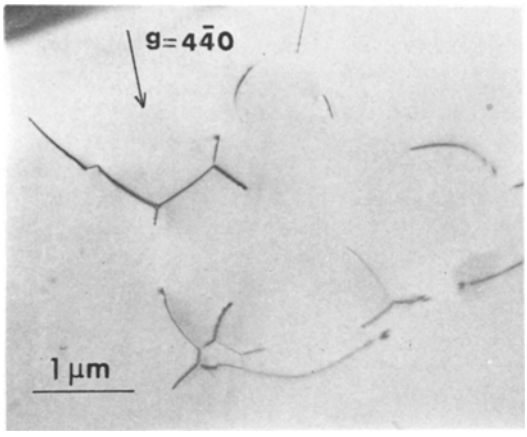

Figure 6 Typical junctions found after 8% creep strain at $T = 1943$ K and $\sigma = 88.2$ MPa. (1 1 1) section.

are blocked into long [0 1 0] straight segments, and slip ceases. Further creep occurs rather by climb, a strain process faster than slip since the latter could only be produced again either by activation of high energy constrictions along faulted ribbons, or by forcing gliding dislocations against a back stress of about $2\gamma_{(1\,0\,\bar{1})}b \geqslant 2\mu/325 = 726$ MPa. Observations of the long time substructures being further support of this view.

3.2.2. Long time substructures

Samples deformed 8% under 88.2 MPa at 1943 K have been observed by TEM. Dislocation density is low, about 10^{11} m^{-2}, but at the scale of TEM almost no subgrain boundary is seen in the foil. A rather uniform distribution of attractive junctions is left, as shown in Fig. 6. Detailed stereographic identifications of the junction arms generally show that climb has occurred in order to reach a 120° equilibrium configuration, so that the plane found for an arm and its Burgers vector is no longer any simple crystallographic plane. Thus only climb configurations appear as a general feature [18].

Berg-Barrett topographs, taken after 5% and 13% creep strains ($T = 1883$ K, $\sigma = 117.6$ MPa) are much the same and confirm, now at the sample scale, the complete absence of any creep cell boundary (see Fig. 7). Only some random subgrain boundaries are seen, locally crossed-over by a few thin, short, extinction contrast lines normal to compression axis. There are probably some erratic small groups of dislocations, connected to the nearby boundary (the source or obstacle for these dislocations), which may be retaining locally the strong ⟨1 0 0⟩ alignment described above.

The lack of any cellular substructure here is in strong contrast with what is observed for the

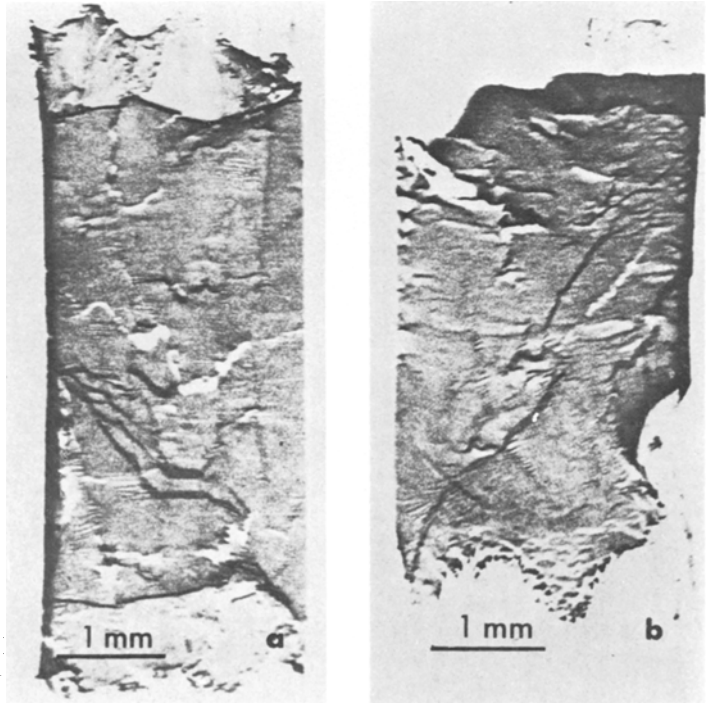

Figure 7 BBT of the (1 0 0) face after different creep strains at 117.6 MPa and 1884 K. g = [4 $\bar{4}$ 0]. (a) 5% creep strain. (b) 13% creep strain.

stoichiometry $n = 1.8$, where it is plausible that creep strain is mainly brought about by glide. If creep strain is due to climb processes, on the other hand, the building up of cell walls is not quite expected.

4. Discussion.

One of the major points to understand is the origin of the remarkable high mechanical strength of stoichiometric spinel, which is reflected here in the high creep strength. Creep rates as low as $10^{-6}\,\mathrm{sec}^{-1}$ are observed, although the temperature is about $0.8\,T_m$ and the stress about $10^{-3}\,\mu$. We think the low diffusion constant of the material is mainly responsible for this. In order to clarify this point, it is useful to compare present results and creep data for $n = 1.8$ found in [5] and [6] with high temperature creep of polycrystalline metals, as is shown in Fig. 8. Following the method of Mukherjee *et al.* [7] the dimensionless quantity $\dot{\epsilon}kT/D_{ox}\mu b$ is plotted versus *resolved* shear stress σ/μ. Here, the resolved shear stress is taken as half the load, and the self-diffusion coefficient D_{ox} is taken from that measured by Ando *et al.* [8] for oxygens ions, since they are probably the slowest moving species, i.e. rate-controlling, in spinels. Fig. 8 shows that the creep strength of spinels is a matter of diffusion constant only, this parameter retaining all the pecularities due to electronic structure. In other respects, the creep behaviour, when properly normalized, is found to be quite comparable to more usual materials. Therefore, instead of Equation 1, the creep law can be written as

$$\dot{\epsilon} = A\,(\sigma/\mu)^m\, D_{ox}\,\mu b/kT \qquad (2)$$

where A and m are dimensionless quantities, and to a first approximation depend only on stoichiometry. The investigated ranges in stress and temperature are too small to give a precise determination of A and m, but m values found in Section 3.1. are consistent with the present plot.

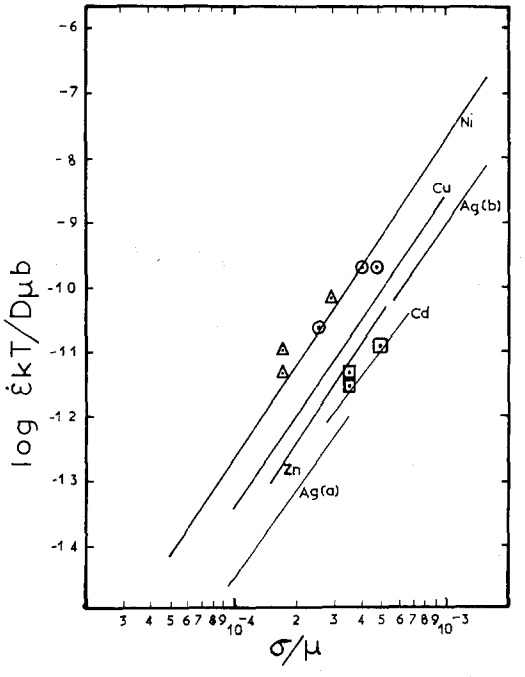

Figure 8 Normalized creep rates versus resolved shear stresses (half of the load). Straight lines stand for high temperature creep data of polycrystalline metals, as quoted in [7]. □ creep of $n = 1.1$. crystals, this work; △ creep of $n = 1.8$ crystals [6] above 1793 K, and ○ below 1793 K [5]. 1793 K is the thermodynamic exsolution temperature of Al_2O_3.

Another point is made apparent from Fig. 8, concerning the stoichiometry effect. It is clear that the factor A becomes at least 10 times larger as n increases from 1.1. to 1.8. We propose that this difference can be rationalized in terms of stacking fault energy. Note, for example, that data for $n = 1.1$. fall on line with straight segments obtained for metals like Ag, Zn, Cd, which are known to have relatively wide split dislocations with stacking faulr energy of the order of $\gamma \simeq \mu b/400$ [7, 12, 13], while data for $n = 1.8$ fall rather on line with nickel, for which $\gamma \simeq \mu b/100$ [7]. At this point we do not claim that there is a straightforward relationship between A and γ. It could just be, for example, that metals of the first group have, because of dissociation, their slip inhibited either as in silver, because of Lomer-Cottrell barriers, or as in zinc or cadmium polycrystals, because of sessile splitting of dislocations on needed prismatic or pyramidal slip systems [12]. Such situations bear some resemblance to the occurrence of sessile dislocations as observed above. Conversely, dislocations in metals like nickel can slip more easily. Similarly the preceding sessile splitting might not occur either in $n = 1.8$ spinels, which seems to be indicated by published works [3, 17]. However no precise stereographic determination of fault plane has been carried out yet; the authors plan to investigate this point further.

In order to account for the effect of stoichiometry on A, let us start from the Orowan creep equation:

$$\dot{\epsilon} = \rho b (L/h) v_c \quad (3)$$

where ρ is the dislocation density ($\rho \sim (\sigma/\mu b)^2$), L the slip distance of a freed dislocation, h the distance to climb in order to free a dislocation and v_c the climb velocity. Since stoichiometry influences only pre-exponential terms like $\rho L/h$, we suggest making $L = h$ in the case of $n = 1$, owing to the inhibition of slip by splitting, making the creep strain a pure climb strain. For $n = 2$ creep is a climb-controlled glide process, so that $L \gg h$, with L being the creep cellular size, for example, as proposed in [5].

Order of magnitude agreements support this view. The usual expression of climb velocity gives here:

$$v_c = 2\pi b (-\ln (2b\rho^{1/2}))^{-1} (D_{ox} \mu b/kT)(\sigma/\mu) \quad (4)$$

Taking the material parameters as previously evaluated, σ as the resolved stress (59 MPa), and $D_{ox} \simeq 10^{-16}\ m^2\ sec^{-1}$ at $T = 1920$ K [8], yields $v_c = 200\ \mu m\ h^{-1} = 5.6 \times 10^{-8}\ m\ sec^{-1}$. With the measured dislocation density $\rho \simeq 10^{11}\ m^{-2}$, $\dot{\epsilon} = \rho b v_c = 3 \times 10^{-6}\ sec^{-1}$. This is just what is read on experimental data (Fig. 2), for the load of 117.6 MPa. Of course, such perfect fit is somewhat fortuitous, due to the rusticity of model, but the order of magnitude agreement shows that pure climb strain can account quantitatively for experimental rates.

Alternatively, if it is accepted that ρ varies as the square of stress, it is clear that a rate equation such as Equation 2 can be predicted with $m = 3$. Fig. 8 gives then $A \simeq 0.1$ for $n = 1.1$. This experimental value compares well with theoretical models of pure climb creep, e.g. Nabarro's model [14] ($A = [\pi \ln (\mu/4\sigma)]^{-1} \simeq 0.05$) or Weertman's model [15] ($A = 0.3$ for $\rho = (\sigma/\mu b)^2$). However it should be emphasized that two parameters are somewhat outside the present experimental precision. Firstly, the experimental stress dependence of creep rate scatters in the range 3 to 4.5, and seems to be slightly larger than 3. Secondly, the experimental creep energy scatters in the range 5 to 6 eV, again slightly larger than the published diffusion energy for oxygen, which is about 4.6 eV [8]. In cases where such differences would really exist (but diffusion measurements are obtained by the not very precise technique of gas–solid exchange utilizing ^{18}O as a tracer), they are balanced by the theoretical coarseness of predictions relative to dislocation climb behaviour, so that they cannot be taken, for the time being, as serious objections to our model.

Our interpretation of the effect of stoichiometry on spinel plasticity is thus fundamentally based on different splitting behaviours, at least as a tentative suggestion which needs further observation. Of course, when compared to other interpretations [2–4], it is of interest to recall that our experimental conditions (strain rates in the range 10^{-6} to $10^{-7}\ sec^{-1}$, resolved shear stresses in the range 0.38 to $0.50 \times 10^{-3}\ \mu$) locate our investigation in the region of a deformation map controlled by dislocation climb, as opposed to the "dislocation glide" region designated by Radford *et al.* [2] and Mitchell *et al.* [4]. It is therefore clear that the dislocation behaviour we observe might concern only processes – deformation mechanisms, preferred slip system – which could be strictly appropriate for the special preceding conditions. For the other cases however, i.e. the high stress/strain rate region, we speculate that the above interpretation might still hold and propose a way to explain various published observations [3, 4, 16, 18].

Mitchell *et al.* [4] have produced 650 kV electron micrographs from a sample strained 0.25% on (1 1 1) slip plane (SFR = 1.43) at 2070 to 2170 K and a constant strain rate $10^{-4}\ sec^{-1}$. Long, straight, edge dislocations similar to the ones we characterized in Fig. 4, are clearly shown (Figs. 3c and f in [4]) but without a precise stereographic identification of dissociation plane. We suggest these might be the remaining, sessile split dislocations developed during early slip in the pre-yield stage and causing harder and harder glide sources to be activated. Hence the slip lines, high dislocation density and work-hardening rate they observe in this stage could be explained. This exhaustion mechanism lasts until stress is high enough to accomodate the imposed strain rate by a climb process only at the test temperature. Once climb has started, dislocations are no longer lying in their slip plane, so that no further glide is possible. Then another (post-yield) deformation stage – a climb stage – takes place. A number of authors [3, 4, 18] have reported that dislocations were rarely observed to lie in well-defined slip planes, in agreement with the preceding view. According to Mitchell *et al.* [4] "climb into lower energy configurations" is occurring under their deformation conditions. They find pieces of crude

dislocation network "with a tendency toward a hexagonal character" quite similar to the 120° junctions formed by climb, as in our Fig. 6. As a result, climb reduces the high dislocation density accumulated during the pre-yield stage (softening, as suggested in [4]), down to values [16] similar to the ones we report in this paper. For such values, extrapolating our data in Fig. 2 shows that strain rates of the order $10^{-4}\,\mathrm{sec}^{-1}$ can be expected in their conditions (2100 K, 172 MPa). Similarly applying Equations 3 and 4 with $L = h$ (pure climb strain), $\rho \simeq 10^{11}\,\mathrm{m}^{-2}$, $D_{ox} \simeq 2 \times 10^{-15}\,\mathrm{m}^2\,\mathrm{sec}^{-1}$ at $T = 2100\,\mathrm{K}$ [8] and $\sigma = 172$ MPa, one computes $\dot{\epsilon} \simeq 1.84 \times 10^{-4}\,\mathrm{sec}^{-1}$ to be compared with their data, $1.4 \times 10^{-4}\,\mathrm{sec}^{-1}$. Moreover, recent precise determination of the dissociation plane performed in this post-yield stage (done on junction arms) show it again distinct from the slip plane [16], the two partials climbing in a way somewhat uncorrelated.

Summarizing, from our creep data we present a deformation picture of stoichiometric spinel in two stages: a first pre-yield slip, followed by a post-yield climb mechanism which develops from sessile split dislocations. It is not unreasonable to extend it to more general mechanical behaviour, at leat as a model designed to stimulate further observations and to achieve a better understanding of stoichiometry effects.

In particular we would not consider $\{1\,1\,1\}\langle 1\,\bar{1}\,0\rangle$ slip as the prevailing easiest slip system for $n = 1$, as it is stated in the literature [2, 4] from limited stress orientation data. We have investigated for the first time the orientation [0 0 1] and shown conclusively from our work that only $\{1\,1\,0\}\langle 1\,\bar{1}\,0\rangle$ slip is activated. On the other hand, $\{1\,1\,1\}\langle 1\,\bar{1}\,0\rangle$ slip is observed for comparable conditions for the [1 1 0] stress orientation, in agreement with Schmid's law. The fact that $\{1\,1\,0\}$ slip is chosen over the $\{1\,1\,1\}$ slip for Schmid factors of 0.5 and 0.41 respectively (ratio 1.22), shows that lattice slip resistance (Peierls forces) on $\{1\,1\,1\}$ planes should not be much smaller than on the $\{1\,1\,0\}$ planes, at most within about 20%, contrary to proposals made up until now [2–4].

References

1. J. HORNSTRA, *J. Phys. Chem. Solids* **15** (1960) 311.
2. K. C. RADFORD and C. W. NEWEY, *Proc. Brit. Ceram. Soc.* **9** (1967) 131.
3. M. H. LEWIS, *Phil. Mag.* **17** (1968) 481.
4. J. E. MITCHELL, L. HWANG and A. H. HEUER, *J. Mater. Sci.* **11** (1976) 264.
5. N. DOUKHAN, R. DUCLOS and B. ESCAIG, *J. Phys.* **34** (1973) C9–379.
6. *Idem ibid.* **37** (1976) C7–566.
7. A. K. MUKHERJEE, J. E. BIRD and J. E. DORN, *Trans. ASM* **62** (1969) 155.
8. K. ANDO and Y. OISHI, *J. Chem. Phys.* **61** (1974) 625.
9. D. J. H. COCKAYNE, *J. Phys.* **35** (1974) C7–141.
10. O. VAN DER BIEST and G. THOMAS, *Phys. Stat. Sol. (a)* **24** (1974) 65.
11. P. VEYSSIERE, J. RABIER and J. GRILHE, *Phys. Stat. Sol. (a)* **31** (1975) 605.
12. J. F. STOHR and J. P. POIRIER, *Phil. Mag.* **25** (1972) 1313.
13. P. B. PRICE, Electron Microscopy and Strength of Crystal, First Berkeley Conference (Interscience, New York, 1963) p. 41.
14. F. R. N. NABARRO, *Phil. Mag.* **16** (1967) 231.
15. J. WEERTMAN, *Trans. ASM* **61** (1968) 681.
16. A. H. HEUER, Private communication.
17. N. DOUKHAN and B. ESCAIG, *J. Phys. Lett.* **35** (1974) L–181.
18. P. VEYSSIERE, J. RABIER, H. GAREM and J. GRILHE, *Phil. Mag.* **33** (1976) 143.

Received 10 October and accepted 16 December 1977.